


ORIGINAL RESEARCH

Open Access



Multi-stage expansion planning of energy storage integrated soft open points considering tie-line reconstruction

Peng Li¹, Jie Ji¹, Sirui Chen², Haoran Ji^{1*} , Jing Xu³, Guanyu Song¹, Jinli Zhao¹, Jianzhong Wu⁴ and Chengshan Wang¹

Abstract

With the rapid development of flexible interconnection technology in active distribution networks (ADNs), many power electronic devices have been employed to improve system operational performance. As a novel fully-controlled power electronic device, energy storage integrated soft open point (ESOP) is gradually replacing traditional switches. This can significantly enhance the controllability of ADNs. To facilitate the utilization of ESOP, device locations and capacities should be configured optimally. Thus, this paper proposes a multi-stage expansion planning method of ESOP with the consideration of tie-line reconstruction. First, based on multi-terminal modular design characteristics, the ESOP planning model is established. A multi-stage planning framework of ESOP is then presented, in which the evolutionary relationship among different planning schemes is analyzed. Based on this framework, a multi-stage planning method of ESOP with consideration of tie-line reconstruction is subsequently proposed. Finally, case studies are conducted on a modified practical distribution network, and the cost–benefit analysis of device and multiple impact factors are given to prove the effectiveness of the proposed method.

Keywords: Active distribution network (ADN), Energy storage integrated soft open points (ESOP), Multi-stage expansion planning, Tie-line reconstruction

1 Introduction

With the extensive integration of distributed generators (DGs), the operating conditions and challenges of active distribution networks (ADNs) are becoming increasingly complex [1]. This makes higher demands on system controllability [2]. To satisfy the flexible operating requirements of ADNs, novel power electronic devices of energy storage (ES) integrated soft open points (ESOP) are employed [3]. As a novel power exchange device based on the fully-controlled power electronic devices [4], ESOP can replace traditional tie-line devices and realize accurate feeder power flow control. With the extra equipped

energy storage, ESOP can provide high-quality flexibility for the operation of distribution systems [5].

SOP integrated with energy storage is promising for improving the operational benefits of distribution networks. It has three main advantages. First, the topology based on back-to-back voltage source converters provides a possibility for combining the SOP and energy storage, as the energy storage battery can be installed at the DC link via a DC-DC converter with a relatively lower investment cost. Second, by controlling the charging and discharging of the energy storage, ESOP further realizes continuous power flow regulation from the spatial–temporal aspects. In addition, the compatible form of ESOP is highly modularized and is suitable for various applications.

Based on the highly modular converter structure, the configuration of ESOP is diversified [6], and the number

*Correspondence: jihaoran@tju.edu.cn

¹ Key Laboratory of Smart Grid of Ministry of Education, Tianjin University, Tianjin 300072, China
Full list of author information is available at the end of the article

of terminals and capacities of each converter can be flexibly designed. Because of the multi-stage expansion requirement of ESOP [7], the integrating location and configured capacities should be considered. Through appropriate device configuration, the flexible power flow regulation ability of ESOP can be fully utilized [8].

SOP-based techniques can play significant roles in distribution networks with high penetration of DGs. Reference [9] proposes a novel optimization method to coordinate SOPs and electric vehicles to effectively promote the maximum hosting capacity of photovoltaic generation in distribution networks. In [10], an efficient conservation voltage reduction (CVR) methodology is proposed based on the coordination of inverter-based DGs and SOPs. Because the location and sizing of SOP have critical impacts on control, in recent years many studies focus on the planning issues of SOP-based devices [11].

To improve the economic benefits of SOPs, reference [12] proposes a two-stage robust model and derives the optimal SOP allocation schemes. In terms of distribution networks with high DG penetration, reference [13] proposes an SOP planning method to reduce the operational cost of ADNs. In fault situations, SOP-based flexible distribution devices can provide voltage support to ensure an uninterrupted power supply [14], while by further considering the reliability of ADNs, a planning method for SOP is proposed in [15] to realize quick supply restoration after natural disasters. In [16], a planning model of SOP is established to maximize the resilience of distribution networks. In addition, the optimal scheme of SOP can also be coordinated with multiple devices [17], while through optimizing the allocation of SOPs and DGs, reference [18] formulates a coordinated planning model to improve the economy, flexibility and controllability of ADNs. In [19], a method is proposed to optimize the locations and sizing of DGs, capacitor banks and SOPs.

As an important flexibility resource, energy storage can be integrated with SOPs to provide a fully-renewable power supply [20]. Compared with the design of original SOPs, ESOPs offer a promising new solution to balance the system power temporally and spatially. Apart from power transfer, ESOPs are capable of regulating feeder power over a time scale. Through charging/discharging of energy storage in ESOP, the temporal and spatial dispatch for renewable energy can be realized. Considering the device coordination of ESOP, reference [21] proposes an ES planning model and obtains a better economic construction scheme, whereas based on the direct current (DC) links of SOPs, a robust scheduling model of ESOP is established to promote energy savings [4].

The above studies mainly focus on the ESOP with a predefined infrastructure. In practical construction, the

configuration of ESOP is more complicated. The number of terminals, integrating location and configured capacity of each converter should be considered comprehensively. However, the existing studies only refer to the limited device configuration schemes, so is difficult to satisfy the flexible operational demands of interconnected ADNs.

To support the rapid growth of system load and renewable energy [22], many studies have looked at the long-term expansion planning problems of ADNs [23]. By restructuring the substations, capacitor banks and voltage regulators, a multi-stage planning method is proposed in [24] to reduce the long-term investment cost. To alleviate the voltage deviation caused by DGs, reference [25] formulates a multi-period planning problem for hybrid AC/DC networks, and while considering DG uncertainties, the various impact factors on network expansion and evolution approach are analyzed [26].

However, traditional planning faces some drawbacks. The physical network is still radial and the adjustment ability of conventional approaches is limited. To satisfy the regulation requirements, such as predefined DG penetration and secure voltage constraints, the resources in different feeders should be controlled cooperatively. With the allocation of ESOP, a flexible and interconnected architecture of the distribution network is established. The configuration of ESOP is also such that it can evolve in different stages to achieve maximum economic benefit. Not only can the equipped capacities of energy storage be expanded in and increasing fashion [27], but the terminal number of ESOP can also be configured flexibly. With the system operating demands varying over a long time-span, the evolutionary relationship among different ESOP planning schemes should be further considered. For example, for a two-terminal SOP, a multi-terminal ESOP can be constructed by further integrating converters and energy storages.

Thus, existing studies on ESOP planning generally refer to device allocation in terms of the present system operational status. However, the optimal location and sizing of ESOP in multiple stages are critical to ensure the flexible and economic operation of ADNs. The long-term capacity expansion and scheduled scheme revolution of ESOP can be further considered. In addition, SOP-based flexible distribution devices are installed to replace conventional tie-lines, although how to reduce the investment cost of ESOP with tie-line reconstruction remains to be investigated.

To address the flexible configuration problem of ESOP, this paper proposes a multi-stage expansion planning

method considering tie-line reconstruction. The main contributions are summarized as follows:

- (1) The multi-stage planning framework of ESOP is formulated, in which the evolutionary process of different planning schemes is elaborated. Based on the multi-terminal modular expansion of ESOP, the flexible distribution devices can be fully used to adapt to the annual growth of DGs and loads.
- (2) An expansion planning model of ESOP is proposed taking into consideration tie-line reconstruction. Through unified planning and multi-stage construction of ESOP, the device investment cost is significantly reduced.

The organization of the rest of the paper is as follows: Sect. 2 establishes the model of a distribution network with ESOP, while Sect. 3 presents the multi-stage expansion method of ESOP. In Sect. 4, the effectiveness of the proposed method is verified, and finally Sect. 5 concludes the paper.

2 Operational modelling of ADN with ESOP

Based on fully-controlled power electronic devices, ESOP can regulate the power flow accurately. With integrated energy storage in DC links, the energy and power injected by DGs can also be effectively transferred from the time point of view. Through regulating ESOP, network loss and voltage deviation can be reduced to support the flexible operation of ADNs with high DG penetration.

2.1 Principle and modelling of ESOP

The main components of ESOP are voltage source AC-DC and DC-DC converters and storage batteries, as shown in Fig. 1. Derived from SOP, ESOP is equipped with energy storage in DC links [28] and realizes the flexible charging/discharging of active power [29].

2.1.1 Multi-terminal converters of ESOP

To meet the diverse operational demands of ADNs, there is a variety of device configurations of ESOP. Compared with the two-terminal SOPs, the number of terminals

of ESOP is not predefined in this paper. With DC links among multiple converters [30], different distribution networks can be interconnected and the device investment cost is more economical. The power transfer constraints of a multi-terminal ESOP are given as:

$$\sum_{i \in \Omega_k} (P_{r,\omega,t,k,i}^{AC} - P_{r,\omega,t,k,i}^{AC,L}) = P_{r,\omega,t,k}^{ES} \quad (1.a)$$

$$P_{r,\omega,t,k,i}^{AC,L} = A_{ac} \sqrt{(P_{r,\omega,t,k,i}^{AC})^2 + (Q_{r,\omega,t,k,i}^{AC})^2} \quad (1.b)$$

$$\sqrt{(P_{r,\omega,t,k,i}^{AC})^2 + (Q_{r,\omega,t,k,i}^{AC})^2} \leq S_{r,k,i}^{AC} \quad (1.c)$$

where $P_{r,\omega,t,k,i}^{AC}$ and $Q_{r,\omega,t,k,i}^{AC}$ denote the active and reactive power injected by ESOP at node i in scheme k and scenario ω at time t during stage r , respectively. $P_{r,\omega,t,k,i}^{AC,L}$ denotes the active power loss of ESOP at node i in scheme k and scenario ω at time t during stage r , while $P_{r,\omega,t,k}^{ES}$ denotes the active power injected by ES of ESOP in scheme k and scenario ω at time t during stage r . $S_{r,k,i}^{AC}$ denotes the capacity of the AC-DC converter at node i in scheme k during stage r .

Among the constraints above, constraint (1.a) represents the relationship of active power transferred by ESOP converters, constraint (1.b) represents the power loss of each converter, and constraint (1.c) denotes the capacity limit of each converter.

2.1.2 Energy storage part of ESOP

Because of the volatility of DG outputs, it is difficult to directly use the generated renewable energy [31]. To enhance the operational complementary capability of ADNs, energy storage can be integrated to provide an efficient power supply for loads [32]. By fast charging/discharging of ES in ESOP, the load demand and renewable energy can be matched in time [33].

Active power injected by each AC-DC converter gathers in DC links and flows into energy storage. The related constraints are:

$$E_{r,\omega,t+1,k}^{ES} - E_{r,\omega,t,k}^{ES} = (P_{r,\omega,t,k}^{ES} - P_{r,\omega,t,k}^{ES,L}) \Delta t \quad (2.a)$$

$$P_{r,\omega,t,k}^{ES,L} = A_{dc} |P_{r,\omega,t,k}^{ES}| \quad (2.b)$$

$$-S_{r,k}^{DC} \leq P_{r,\omega,t,k}^{ES} \leq S_{r,k}^{DC} \quad (2.c)$$

$$SOC_{min}^{ES} S_{r,k}^{BA} \leq E_{r,\omega,t,k}^{ES} \leq SOC_{max}^{ES} S_{r,k}^{BA} \quad (2.d)$$

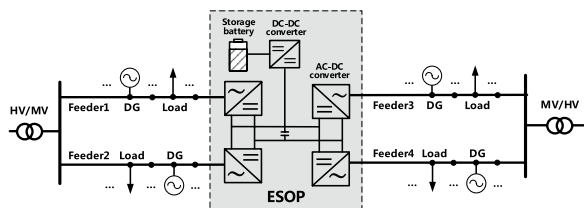


Fig. 1 Structure of ESOP with multi-terminal converters

$$E_{r,\omega,t_N,k}^{\text{ES}} = E_{r,\omega,t_0,k}^{\text{ES}} \quad (2.e)$$

where $E_{r,\omega,t,k}^{\text{ES}}$ and $P_{r,\omega,t,k}^{\text{ES,L}}$ denote energy stored by ES of ESOP and the power loss of ES in scheme k and scenario ω at time t during stage r , respectively. $S_{r,k}^{\text{DC}}$ and $S_{r,k}^{\text{BA}}$ denote the respective capacities of DC-DC converter and storage battery in scheme k during stage r .

Constraint (2.a) represents the relationship between the injected power and stored energy in ES, while constraint (2.b) represents the power loss of DC-DC converters. Constraints (2.c) and (2.d) represent the limit of injected power and stored energy of ES, respectively. Constraint (2.e) is added to ensure the consistency of stored energy status in ES.

2.2 Operational modelling of ADN with ESOP

With the integration of ESOP, the operating status of ADNs can be significantly improved. AC-DC converters have the capability of accurate power flow control, which can efficiently reduce network loss and voltage deviation. Various DC-powered devices can be integrated into the DC links of ESOP. This facilitates the coordination of AC/DC hybrid distribution networks.

2.2.1 Power flow model of distributed networks

BY adopting the DistFlow model, the power flow constraints of ESOP-based distribution networks are shown as follows:

$$\sum_{ij \in \mathcal{L}_{\text{all}}} (P_{r,\omega,t,ij} - r_{ij} l_{r,\omega,t,ij}) + P_{r,\omega,t,j} = \sum_{jg \in \mathcal{L}_{\text{all}}} P_{r,\omega,t,jg} \quad (3.a)$$

$$\sum_{ij \in \mathcal{L}_{\text{all}}} (Q_{r,\omega,t,ij} - x_{ij} l_{r,\omega,t,ij}) + Q_{r,\omega,t,j} = \sum_{jg \in \mathcal{L}_{\text{all}}} Q_{r,\omega,t,jg} \quad (3.b)$$

$$v_{r,\omega,t,i} - v_{r,\omega,t,j} + (r_{ij}^2 + x_{ij}^2) l_{r,\omega,t,ij} - 2(r_{ij} P_{r,\omega,t,ij} + x_{ij} Q_{r,\omega,t,ij}) = 0 \quad (3.c)$$

$$P_{r,\omega,t,ij}^2 + Q_{r,\omega,t,ij}^2 = v_{r,\omega,t,i} l_{r,\omega,t,ij} \quad (3.d)$$

$$P_{r,\omega,t,i} = P_{r,\omega,t,i}^{\text{DG}} + \sum_{k \in \mathcal{L}} P_{r,\omega,t,k,i}^{\text{AC}} - P_{r,\omega,t,i}^{\text{LD}} \quad (3.e)$$

$$Q_{r,\omega,t,i} = Q_{r,\omega,t,i}^{\text{DG}} + \sum_{k \in \mathcal{L}} Q_{r,\omega,t,k,i}^{\text{AC}} - Q_{r,\omega,t,i}^{\text{LD}} \quad (3.f)$$

where $P_{r,\omega,t,ij}$ and $Q_{r,\omega,t,ij}$ denote the respective active and reactive power flow of line ij in scenario ω at time t during stage r . $P_{r,\omega,t,i}$ and $Q_{r,\omega,t,i}$ denote the total active and reactive power injection at node i in scenario ω at time t during stage r , respectively. $l_{r,\omega,t,ij}$ and $v_{r,\omega,t,j}$ denote the respective squared voltage magnitude of node i and

current magnitude of branch ij in scenario ω at time t during stage r .

The secure limits of nodal voltage and line current are shown as constraints (4.a) and (4.b), as:

$$(U_i^{\text{min}})^2 \leq v_{r,\omega,t,i} \leq (U_i^{\text{max}})^2 \quad (4.a)$$

$$l_{r,t,ij} \leq (I_{ij}^{\text{max}})^2 \quad (4.b)$$

where U_i^{min} and U_i^{max} denote the lower and upper limits of voltage at node i , while I_{ij}^{max} denotes the maximum loading current of line ij .

2.2.2 Operational model of DGs

Taking photovoltaic and wind turbines as examples [34], the operational model of DG can be described as:

$$0 \leq P_{r,\omega,t,i}^{\text{DG}} \leq \bar{P}_{r,t,i}^{\text{DG}} \quad (5.a)$$

$$\left| Q_{r,\omega,t,i}^{\text{DG}} \right| \leq \frac{P_{r,t,i}^{\text{DG}} \sqrt{1 - (\mu_i^{\text{min}})^2}}{\mu_i^{\text{min}}} \quad (5.b)$$

$$\sqrt{(P_{r,\omega,t,i}^{\text{DG}})^2 + (Q_{r,\omega,t,i}^{\text{DG}})^2} \leq S_i^{\text{DG}} \quad (5.c)$$

where $P_{r,\omega,t,i}^{\text{DG}}$ and $Q_{r,\omega,t,i}^{\text{DG}}$ are the respective active and reactive power injected by DG at node i in scenario ω at time t during stage r . $\bar{P}_{r,t,i}^{\text{DG}}$ is the maximum power output of DG at node i at time t during stage r , S_i^{DG} is the capacity of DG i , and μ_i^{min} is the power factor of DG i .

3 Mathematical formulation of multi-stage expansion planning for ESOP

Given the multi-terminal modular characteristics of ESOP, the practical design should allow for the principle of unified planning and multi-stage construction. Apart from the demand for expanding networks, the terminal number and integrating location of ESOP should be further considered. By reasonably arranging the detailed ESOP construction scheme, flexible distribution devices can be economically used.

3.1 Framework of the multi-stage planning of ESOP

In the initial stage, it is essential to formulate the ESOP construction schemes with available integrating nodes. The scheme information includes the number of terminals of ESOP and the integrating location of converters. During the multi-stage construction, the number of terminals can be increased. For example, a two-terminal

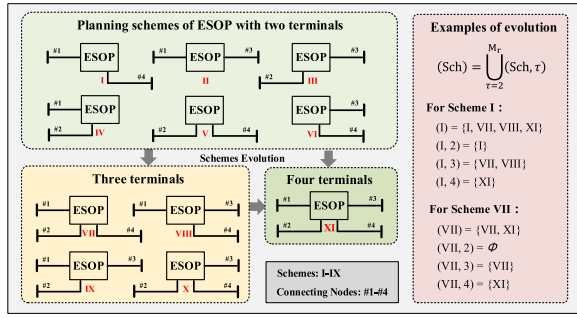


Fig. 2 Planning framework of ESOP in multiple stages

ESOP can evolve into three terminals or more. Energy storage can be integrated into the DC links of ESOP at any stage. The relationship between the different ESOP planning schemes is described in Fig. 2.

There are four nodes that are available to access converters in Fig. 2, namely #1, #2, #3, and #4. Therefore, six planning schemes of ESOP with two terminals are constructed. Then, three-terminal and four-terminal topologies of ESOP evolve based on the previous structures. Taking Scheme I for instance, the total evolved ESOP planning schemes can be presented as (I) = {I, VII, VIII, XI}. The subset of the two-terminal ESOP planning scheme only includes itself, which is described as (I, 2) = {I}. The subset of the three-terminal ESOP planning schemes is described as (I, 3) = {VII, VIII}, in which the schemes contain both nodes #1 and #4. The subset of the four-terminal ESOP planning schemes is described as (I, 4) = {XI}.

$$\mathcal{L} = \bigcup_{k=1}^{N_k} \mathcal{L}(k) = \bigcup_{k=1}^{N_k} \bigcup_{\tau=2}^{M_r} \mathcal{L}(k, \tau) \quad (6.a)$$

$$\mathcal{L}(k, 2) = \{k | \text{size}(\Omega_k) = 2\} \quad (6.b)$$

$$\mathcal{L}(k, 3) = \{h | \text{size}(\Omega_h) = 3, \Omega_h \supseteq \Omega_k, k \in \mathcal{L}(k, 2)\} \quad (6.c)$$

$$\mathcal{L}(k, 4) = \{p | \text{size}(\Omega_p) = 4, \Omega_p \supseteq \Omega_h, h \in \mathcal{L}(k, 3)\} \quad (6.d)$$

In (6.a)–(6.d), M_r denotes the maximum ESOP terminal number. $\mathcal{L}(k)$ and $\mathcal{L}(k, \tau)$ are the sets of ESOP and τ -terminal ESOP planning schemes evolved from scheme k , respectively. Function $\text{size}(\Omega_k)$ denotes the nodes number of scheme k .

During practical construction, the multi-stage planning schemes should allow the following constraints:

$$\sum_{h \in \mathcal{L}(k)} \alpha_{r,h} \leq 1, \forall k \in \mathcal{L} \quad (7.a)$$

$$S_{r-1,k}^{AC} \leq \sum_{h \in \mathcal{L}(k)} S_{r,h}^{AC} \quad (7.b)$$

$$S_{r-1,k}^{DC} \leq \sum_{h \in \mathcal{L}(k)} S_{r,h}^{DC} \quad (7.c)$$

$$\eta S_{r-1,k}^{BA} \leq \sum_{h \in \mathcal{L}(k)} S_{r,h}^{BA} \quad (7.d)$$

where η is the damping coefficient of storage battery capacity, and $\alpha_{r,h}$ is a binary variable, which denotes the selection of scheme h during stage r , and scheme $h \in \mathcal{L}(k)$ is evolved from scheme k . Constraint (7.a) ensures the uniqueness of scheme selection, and avoids multiple ESOPs connecting to one node, while constraints (7.b) to (7.d) represent the expansive relationship of scheduled device capacities at different stages. In detail, the capacities of the AC-DC and DC-DC converters and storage battery during stage r , are required to be no less than the corresponding capacities during the former stage $r - 1$.

3.2 Expansion planning model of ESOP with tie-line reconstruction

Based on the ESOP expansion framework, a multi-stage expansion planning model of ESOP can be established taking into consideration tie-line reconstruction. Through constructing ESOP over a long period of time, the device investment cost is expected to be reduced.

3.2.1 Objective function

The objective function of the ESOP expansion model is given as:

$$\min f = \sum_{r=1}^{N_r} T_r f_r \quad (8.a)$$

$$f_r = f_r^d + f_r^s + f_r^m + f_r^b + f_r^l \quad (8.b)$$

where T_r denotes the period of planning stage r . f_r^d , f_r^s , f_r^m , f_r^b and f_r^l denote the annual costs of ESOP device investment, land expropriation, ESOP device maintaining, tie-line reconstruction and power loss, respectively.

In practical construction, the device investment cost of ESOP has a relationship with the expansion capacities in each planning stage. Considering the price fluctuation, the annual device investment cost of ESOP can be described as:

$$f_r^d = \sum_{r'=1}^r \left(f_{r'}^{d,ESOP} - f_{r'-1}^{d,ESOP} + \Delta f_{r'}^{BA} \right) \quad (9.a)$$

$$f_{r'}^{d,ESOP} = \frac{d(1+d)^y}{(1+d)^y - 1} \sum_{k \in \mathcal{L}} \left(c_{r',k}^{AC} S_{r',k}^{AC} + c_{r',k}^{DC} S_{r',k}^{DC} + c_{r',k}^{BA} S_{r',k}^{BA} \right) \quad (9.b)$$

$$\Delta f_{r'}^{BA} = c_{r'}^{BA} \frac{d(1+d)^y}{(1+d)^y - 1} (1-\eta) S_{r'-1,k}^{BA} \quad (9.c)$$

where $c_{r'}^{AC}$, $c_{r'}^{DC}$ and $c_{r'}^{BA}$ denote the device capacity investment prices per unit of AC-DC converter, DC-DC converter and storage battery, respectively. Parameters of the discount rate d and device lifetime y are introduced to take the future value variations of investment cost into consideration. $\Delta f_{r'}^{BA}$ denotes the investment cost caused by the capacity reduction of the storage battery.

The annual costs of land expropriation, ESOP maintenance and tie-line reconstruction are:

$$f_r^s = \frac{d(1+d)^y}{(1+d)^y - 1} \sum_{r'=1}^r \sum_{k \in \mathcal{L}} c_{r'}^{\text{site}} (\alpha_{r',k} - \alpha_{r'-1,k}) \quad (10.a)$$

$$f_r^m = \sum_{k \in \mathcal{L}} c_r^m (S_{r,k}^{AC} + S_{r,k}^{DC} + S_{r,k}^{BA}) \quad (10.b)$$

$$f_r^b = \frac{d(1+d)^y}{(1+d)^y - 1} \sum_{r'=1}^r \sum_{k \in \mathcal{L}} c_{r'}^L \xi \alpha_{r',k} L_k^n \quad (10.c)$$

where $\alpha_{r',k}$ is a binary variable which denotes the selection of scheme k during stage r' . When $\alpha_{r',k}$ equals 1, the construction plan is determined as scheme k . $c_{r'}^{\text{site}}$, c_r^m and $c_{r'}^L$ denote the land expropriation price, maintaining price and line construction price, respectively. ξ is the terrain correction coefficient, and L_k^n is the line length to be constructed in scheme k .

The power loss of ADNs includes network loss and device loss, which can be described as:

$$f_r^l = 365 \sum_{\omega=1}^{N_\omega} \sum_{t=1}^{N_t} c_{r,t}^p p_\omega (P_{r,\omega,t}^{\text{Line}} + P_{r,\omega,t}^{\text{Dev}}) \Delta t \quad (11.a)$$

$$P_{r,\omega,t}^{\text{Line}} = \sum_{ij \in \uparrow_{\text{all}}} r_{ij} l_{r,\omega,t,ij} \quad (11.b)$$

$$P_{r,\omega,t}^{\text{Dev}} = \sum_{k \in \mathcal{L}} \left(\sum_{i \in \Omega_k} P_{r,\omega,t,k,i}^{\text{AC,L}} + P_{r,\omega,t,k}^{\text{ES,L}} \right) \quad (11.c)$$

where $c_{r,t}^p$ is the time-of-use (ToU) electricity price at time t during stage r , and p_ω is the probability of scenario ω .

3.2.2 Planning constraints of ESOP

The ESOP planning constraints consist of the capacity limits on AC-DC and DC-DC converters and storage batteries, as:

$$S_{r,k}^{AC} = \sum_{i \in \Omega_k} S_{r,k,i}^{AC} \quad (12.a)$$

$$\alpha_{r,k} \varepsilon \leq S_{r,k}^{AC} \leq \alpha_{r,k} M \quad (12.b)$$

$$0 \leq S_{r,k}^{DC} \leq \alpha_{r,k} M, 0 \leq S_{r,k}^{BA} \leq \alpha_{r,k} M \quad (12.c)$$

Constraint (12.a) represents the total capacities of all AC-DC converters, while constraints (12.b) and (12.c) represent the capacity limits of each ESOP component. Variable $\alpha_{r,k}$ refers to whether the AC-DC converters of ESOP are equipped or not. With the binary variable $\alpha_{r,k}$, the operating constraints of ESOP can be transformed as:

$$\alpha_{r,k} \left[\sum_{i \in \Omega_k} (P_{r,\omega,t,k,i}^{AC} - P_{r,\omega,t,k,i}^{AC,L}) - P_{r,\omega,t,k}^{ES} \right] = 0 \quad (13)$$

When $\alpha_{r,k}$ equals 1, it is essential to equip with AC-DC converters, and (13) is identical to (1.a). When $\alpha_{r,k}$ equals 0, AC-DC converters are not equipped, making the relationship of active power transformation ineffective. The construction of DC-DC converters and storage batteries is implemented according to the practical demands of ADNs.

In addition, the scheme evolution constraints of ESOP should be considered. The detailed constraints are given in constraints (6) and (7).

3.2.3 Constraints of renewable energy penetration

With the growth of installed DGs, the penetration of renewable energy generation continues to increase. However, the DG outputs come with serious uncertainty and intermittence, which may lead to electricity curtailment. To effectively enhance the DG penetration, it is necessary to determine the DG location and set a proper target for renewable energy generation in advance. Thus, the following constraint is added:

$$\sum_{t=1}^{N_t} \sum_{i \in \Omega_{\text{all}}} (P_{r,\omega,t,i}^{\text{DG}} - \gamma_r P_{r,\omega,t,i}^{\text{LD}}) \geq 0 \quad (14)$$

where γ_r denotes the pre-set index of DG penetration during stage r .

3.2.4 Constraints of active distribution networks

The constraints of distribution networks include the power flow constraints and the secure operation constraints, which are given as constraints (3) and (4).

3.3 Modelling conversion and solution methodology

Because of the non-convexity and nonlinearity of the ESOP planning model, the problem posed above is difficult to solve. By adopting the method of convex relaxation, the related constraints (1.b), (1.c) and (3.d) can be transformed as:

$$\left\| \begin{matrix} P_{r,\omega,t,k,i}^{AC} \\ Q_{r,\omega,t,k,i}^{AC} \end{matrix} \right\| \leq S_{r,k,i}^{AC} \left\| \begin{matrix} P_{r,\omega,t,k,i}^{AC} \\ Q_{r,\omega,t,k,i}^{AC} \end{matrix} \right\| \leq A_{ac} P_{r,t,i}^{AC,L} \quad (15.a)$$

$$\left\| \begin{matrix} 2P_{r,\omega,t,ij} \\ 2Q_{r,\omega,t,ij} \\ l_{r,\omega,t,ij} - v_{r,\omega,t,i} \end{matrix} \right\| \leq l_{r,\omega,t,ij} + v_{r,\omega,t,i} \quad (15.b)$$

As for the absolute constraint (2b), the following constraints are added:

$$P_{r,\omega,t,k}^{ES,L} \geq A_{dc} P_{r,\omega,t,k}^{ES}, P_{r,\omega,t,k}^{ES,L} \geq -A_{dc} P_{r,\omega,t,k}^{ES} \quad (16)$$

The nonlinear constraint (13) can be converted to constraints (17.a) and (17.b), as:

$$(\alpha_{r,k} - 1)M \leq \sum_{i \in \Omega_k} (P_{r,\omega,t,k,i}^{AC} - P_{r,\omega,t,k,i}^{AC,L}) - P_{r,\omega,t,k}^{ES} \quad (17.a)$$

$$\sum_{i \in \Omega_k} (P_{r,\omega,t,k,i}^{AC} - P_{r,\omega,t,k,i}^{AC,L}) - P_{r,\omega,t,k}^{ES} \leq (1 - \alpha_{r,k})M \quad (17.b)$$

In summary, the ESOP planning model can be converted to the following mixed-integer second-order cone programming (MISOCP) model [35]:

$$\begin{aligned} \min f &= \sum_{r=1}^{N_r} Tr(f_r^d + f_r^s + f_r^m + f_r^b + f_r^l) \\ \text{s.t.} &\begin{cases} (1.a), (2.a), (2.c) - (2.e), (3.a) \\ (3.c) - (3.f), (4) - (12), (14) - (17) \end{cases} \end{aligned} \quad (18)$$

4 Case studies and analysis

To verify the effectiveness of the proposed method, case studies are conducted by a CPLEX 12.8 solver interfaced with a YALMIP toolbox. The optimization test environment is a PC with an Intel (R) Core (TM) i7-12,700 CPU @ 2.10 GHz and 16 GB RAM.

4.1 Modified practical distribution networks

Case studies are conducted based on the modified practical network in Taiwan [36]. The network contains three 11.4 kV feeders and two existing tie-lines, as shown in Fig. 3. There are eight nodes available to access converters, and these are marked as red points in Fig. 3. Before the initial planning, the total system loads are 7.54 MW and 5.23 Mvar, respectively. The installed PV capacities are 4.8 MWp. By adopting the k-means method, the local historical data of DGs and loads are clustered into 3 typical scenarios. The operation curves of the initial stage are shown in Fig. 4.

The device expansion is implemented in four stages and each stage lasts for five years. During the four

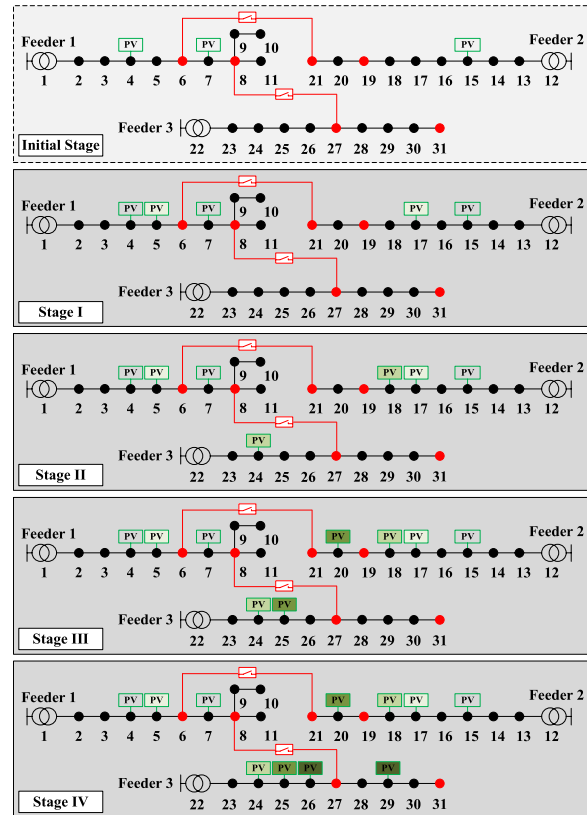


Fig. 3 Structure of the modified practical distribution network

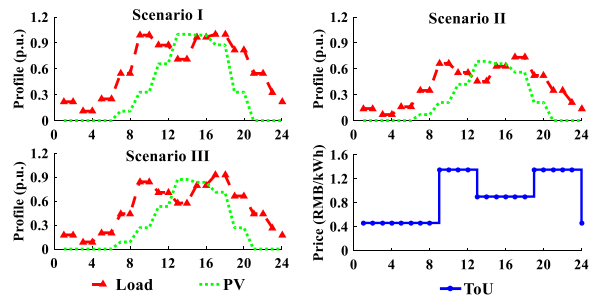


Fig. 4 Curves of load, PV generation and ToU electricity price

stages, the penetration of renewable energy generation increases, and the location of the newly-installed DG in each stage is shown in Fig. 3. The variations of ESOP investment price, system load and DG accommodation in four stages are given in Tables 1 and 2 [36]. The discount rate is set at 0.08, while the lower and upper voltage limits are set to 0.95 p.u. and 1.05 p.u., respectively [37]. The ES state of charge remains at [20%, 90%], and it is assumed that the capacity of the storage battery is reduced by 2% annually. Based on the predicted daily electricity demand and DG generation,

Table 1 Price parameters of various devices

Price	Stage I	Stage II	Stage III	Stage IV
AC-DC converter price (RMB/kVA)	1000	800	600	500
DC-DC converter price (RMB/kW)	500	400	350	300
Storage battery price (RMB/kWh)	500	400	350	300
ESOP maintaining price (RMB)	60	80	100	120
Line constructing price (10 ⁴ RMB/km)	10	12	16	20
Land expropriation price (10 ⁴ RMB)	500	550	600	700
DG generation price (RMB/kWh)	0.25	0.22	0.17	0.15

Table 2 Growth parameters of load and DG

Parameters	Stage I	Stage II	Stage III	Stage IV
Annual load growth rate (%)	4	3	1.5	1.0
Peak load (MW)	9.17	10.63	11.46	12.04
DG accommodation (MWp)	6.80	9.80	12.80	16.80
Daily electricity demand (MWh)	63.11	73.17	78.82	82.84
Daily DG generation (MWh)	27.34	39.40	51.46	67.54
DG penetration (%)	42	52	64	80

the maximum ratios of renewable energy generation in the four stages can be evaluated, and the indices of DG penetration are set to 42%, 52%, 64% and 80%, respectively [38].

4.2 Planning result and cost-benefit analysis of ESOP

Considering the load increment, DG expansion and investment price reduction, ESOP planning is carried out over a long time horizon. By constructing ESOP with existing tie-lines, the investment cost can be significantly reduced. Through multi-stage ESOP planning, the varying operational demands of ADNs are satisfied.

4.2.1 Planning result of ESOP in multiple stages

Case I The multi-stage ESOP expansion planning is implemented by adopting the proposed planning method.

The planning results of Case I are shown in Fig. 5. It can be seen that, on basis of the tie-line between nodes 8 and 27, a two-terminal ESOP is constructed at the first planning stage. At stage II, the third AC-DC converter is scheduled based on the existing two-terminal ESOP. The three feeders are interconnected with only one new line, which significantly reduces the investment cost. Moreover, through multi-stage ESOP construction, a better

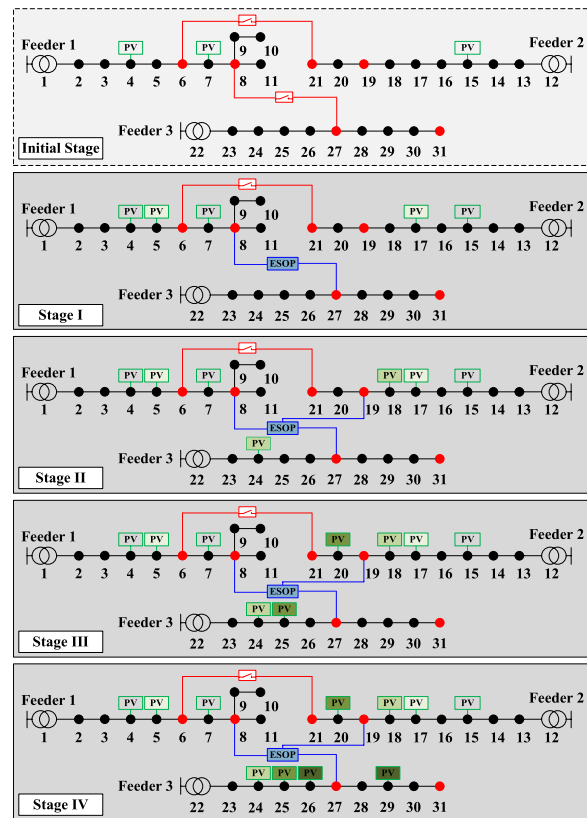


Fig. 5 Planning results of the network based on ESOP in Case I

Table 3 Planning capacity of ESOP in Case I

Scheduled capacity	Stage I	Stage II	Stage III	Stage IV
<i>AC-DC converter (MVA)</i>				
Node 8	1.53	1.53	1.77	2.04
Node 19	–	0.48	2.11	2.13
Node 27	0.79	0.79	1.38	5.19
DC-DC converter (MW)	0.71	1.83	4.39	7.99
Storage battery (MWh)	2.02	5.18	16.77	45.15

adaptation of the shifts of increasing DG shares can be obtained (Table 2).

The scheduled capacities in the four stages are given in Table 3. Considering the increment of tie-line investment cost, early construction may lead to superiority in device price. The results show that tie-line reconstruction is implemented at stage II. This can reduce the long-term investment cost. To facilitate DG penetration, the capability of power transfer needs to be strengthened [39]. Thus, the capacities of ESOP are expanding in the four stages. Energy storage is assembled to realize the complementarity of DG outputs and system loads. Table 4 shows the multi-stage investment

Table 4 Multi-stage investment cost in Case I

Annual cost (10 ⁴ RMB)	Stage I	Stage II	Stage III	Stage IV
ESOP device cost	37.49	62.00	157.88	449.48
Land expropriation cost	50.93	50.93	50.93	50.93
Maintaining cost	3.03	7.85	26.43	75.00
Power loss cost	38.79	41.56	45.34	63.25
Line construction cost	0.00	12.93	12.93	12.93
Total investment cost	130.24	178.29	304.37	688.89

cost in Case I. It can be seen that the land expropriation cost and tie-line construction cost are charged within stages I and II. With the capacity expansion of ESOP converters, the maintenance cost increases simultaneously.

4.2.2 Cost–benefit analysis of ESOP

To analyze the economic benefits of device investment, the following Case II is added.

Case II The operational results are obtained with no consideration of ESOP construction.

Through integrating ESOP, the system operational status can be significantly improved. The cost-benefits of ESOP are derived from the decrement in electricity purchase cost, power loss cost, voltage deviation punishing cost and DG curtailment punishing cost. The voltage deviation punishing cost and DG curtailment punishing cost are shown as:

$$f_r^v = 365 \cdot \lambda \sum_{t=1}^{N_t} \sum_{i \in \Omega_{all}} |U_{r,t,i}^2 - U_0^2| \quad (19.a)$$

$$f_r^c = 365 \cdot c_r^{DG} \sum_{t=1}^{N_t} \sum_{i \in \Omega_{all}} (\bar{P}_{r,t,i}^{DG} - P_{r,t,i}^{DG}) \quad (19.b)$$

where λ denotes the punishing coefficient of voltage deviation, which is set to 10, and c_r^{DG} denotes the electricity generation price of DGs during stage r .

Thus, the total cost of ADNs with ESOP is:

$$f_r^T = f_r + f_r^e + f_r^v + f_r^c \quad (20)$$

where f_r^e is the annual electricity purchase cost during stage r .

The cost–benefit results in multiple stages are given in Table 5. With the ESOP price reduction and DG accommodation increment, the system operational benefits derived from ESOP are higher than the device investment cost. At stage I, the annual total investment cost is 1.30×10^6 RMB and the total cost is reduced by 1.27×10^6 RMB each year. It means that most of ESOP investment costs can be recovered. With increase in the installed DGs, the annual electricity purchase cost and the total cost are continuously reduced. At stage IV, the total cost is reduced by 9.61×10^6 RMB, which is significantly higher than the investment cost. It proves that multi-stage planning can improve the benefits of ESOP construction.

4.3 Impact factor analysis of ESOP planning

IN practical long-period ESOP construction, device configuration is determined by multiple factors. Thus, the following planning analysis is conducted to determine the main impact factors, including tie-line location, renewable energy penetration requirement and device investment cost fluctuation.

Table 5 Cost–benefit result in multiple stages

Annual cost (10 ⁴ RMB)	Electricity purchase cost	Power loss cost	Voltage deviation cost	DG curtailment cost	Total investment cost	Total cost
<i>Stage I</i>						
Case I	2556.12	38.79	6.29	2.88	130.24	2695.53
Case II	2730.63	44.93	8.04	38.50	–	2822.10
<i>Stage II</i>						
Case I	2440.32	41.56	6.20	9.12	178.29	2633.93
Case II	2628.55	52.09	8.37	36.01	–	2725.02
<i>Stage III</i>						
Case I	1936.37	45.34	5.40	2.06	304.37	2248.20
Case II	2485.24	56.23	8.38	80.15	–	2630.00
<i>Stage IV</i>						
Case I	1122.13	63.25	4.09	0.98	688.89	1816.09
Case II	2511.90	61.26	8.46	196.30	–	2777.92
<i>Total stages</i>						
Case I	8,054.94	188.94	21.98	15.04	1,301.79	9,393.75
Case II	10,356.32	214.51	33.25	350.96	–	10,955.04

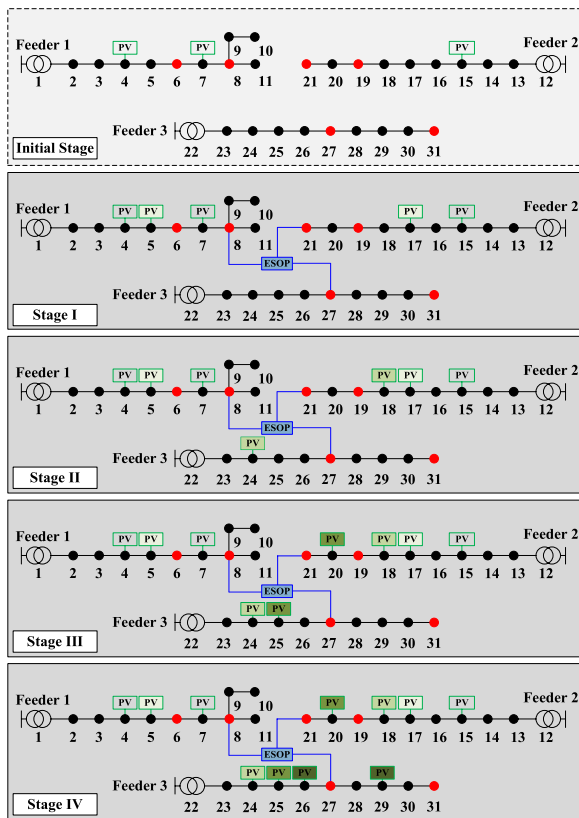


Fig. 6 Planning result of the network based on ESOP in Case III

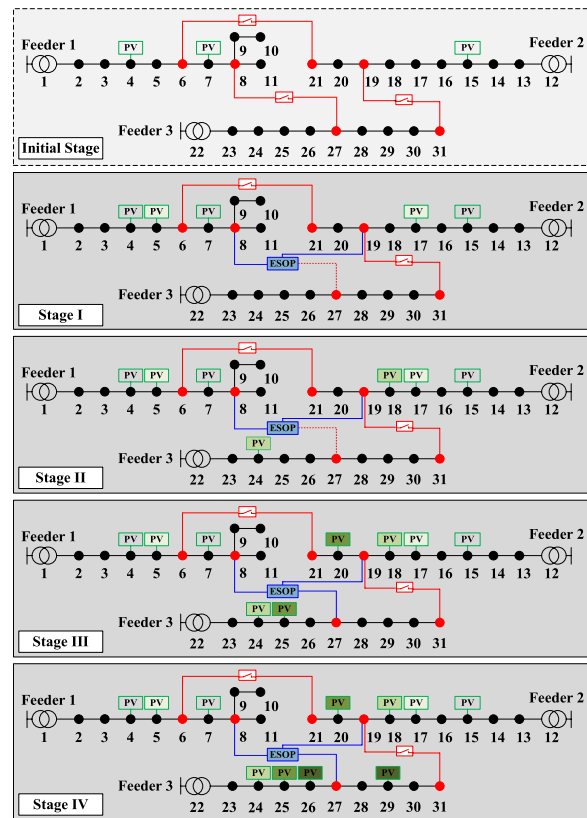


Fig. 7 Planning results of the network based on ESOP in Case IV

4.3.1 Location of tie-lines

Two cases with different initial network structures are added.

Case III The multi-stage ESOP expansion planning is implemented by adopting the proposed planning method. The initial network has no existing tie-line.

Case IV The multi-stage ESOP expansion planning is implemented by adopting the proposed planning method. The initial network has three tie-lines at nodes 6–21, nodes 8–27 and nodes 19–31.

Figures 6 and 7 show the planning results of the network based on ESOP in Case III and IV, respectively. The blue solid line presents a power transformation path of ESOP, where the converters have been allocated at the current stage. The red dashed line connecting ESOP presents the original tie switch line, which will be reconstructed with converters at later stages for power transmission.

The ESOP planning capacities and cost–benefit for Case III are given in Table 6. It can be seen that the scheduled capacities in Case I and Case III are analogous. The former has a reduction of tie-line investment costs each year of approximately 1.32×10^5 RMB.

With different tie-line locations, the ESOP planning scheme has an alternative. By assembling converters at nodes 8, 19 and 27, a three-terminal ESOP is constructed between the three feeders. The results in Fig. 7 and Table 7 for Case IV show that by reconstructing tie-lines, the device investment cost can be reduced. Also, the location has a relationship with the selection of planning schemes.

4.3.2 Requirement of DG penetration in ADNs

The capacities of DGs increase during the four stages, while the installed DGs are located at different feeders. Assuming that the four planning stages have different DG penetration requirements, the following case is added:

Case V Multi-stage ESOP expansion planning is implemented by adopting the proposed planning method. The requirements for renewable energy penetration in the four stages are set to 30%, 45%, 60% and 80%, respectively.

The selected ESOP planning scheme is depicted in Fig. 8 and the scheduled capacities are given in Table 8. With tie-lines between nodes 8 and 27, feeders are interconnected by ESOP among nodes 8, 21 and 27. The converter capacities are expanded within the four stages. With a lower requirement of DG penetration in the prior

Table 6 Multi-stage planning results in Case III

Result	Stage I	Stage II	Stage III	Stage IV
<i>AC-DC converter (MVA)</i>				
Node 8	1.52	1.52	1.77	2.05
Node 21	0.02	0.48	2.08	2.13
Node 27	0.76	0.76	1.41	5.20
DC-DC converter (MW)	0.72	1.83	4.39	8.00
Storage battery (MWh)	2.05	5.18	16.77	45.16
Line construction cost (10^4 RMB)	13.18	13.18	13.18	13.18
Total investment cost (10^4 RMB)	146.05	180.85	307.66	692.76
Total cost (10^4 RMB)	2712.96	2636.06	2251.12	1827.44

Table 7 Multi-stage planning results in Case IV

Result	Stage I	Stage II	Stage III	Stage IV
<i>AC-DC converter (MVA)</i>				
Node 8	1.54	1.52	1.77	2.04
Node 19	0.55	0.59	2.12	2.13
Node 27	–	–	1.37	5.19
DC-DC converter (MW)	1.50	1.83	4.39	7.99
Storage battery (MWh)	4.24	5.44	16.77	45.15
Line construction cost (10^4 RMB)	8.21	8.21	10.97	10.97
Total investment cost (10^4 RMB)	154.33	171.69	304.91	689.46
Total cost (10^4 RMB)	2711.29	2627.29	2248.84	1816.72

Table 8 Multi-stage planning results in Case V

Result	Stage I	Stage II	Stage III	Stage IV
<i>AC-DC converter (MVA)</i>				
Node 8	0.73	1.42	1.73	2.05
Node 21	–	0.05	0.60	2.11
Node 27	0.08	0.12	0.55	5.21
DC-DC converter (MW)	–	–	2.17	8.00
Storage battery (MWh)	–	–	8.60	45.17
Total investment cost (10^4 RMB)	99.69	122.62	203.52	700.26
Total cost (10^4 RMB)	2865.54	2788.39	2405.29	1834.95

stages, the scheduled scales of AC-DC converter capacity are relatively small. Compared with Case I, it is not necessary to equip with energy storage at stages I and II.

It can be concluded that the ESOP planning results are related to the requirements of DG penetration. At the initial stage, the installed DG is small, and the equipped AC-DC converters are responsible for the feeder power flow control. With the increment of DG penetration, energy storage is integrated into the DC links of ESOP to improve energy efficiency. It can also be seen that the higher DG penetration requirements lead to larger ES capacities.

From the results given in Table 8, the cost–benefit is influenced by the scheduled capacity in each stage. At the initial planning stage in Case V, the scheduled converter capacities are on a small scale. Compared with Case I, the total costs in Case V are increased by 4.34×10^5 RMB and 6.34×10^5 RMB at the first two stages. With the scheduled capacity increase, the cost benefits turn positive and the cost reduction is 9.43×10^6 RMB at Stage IV. It indicates that early ESOP construction can facilitate device investment recovery.

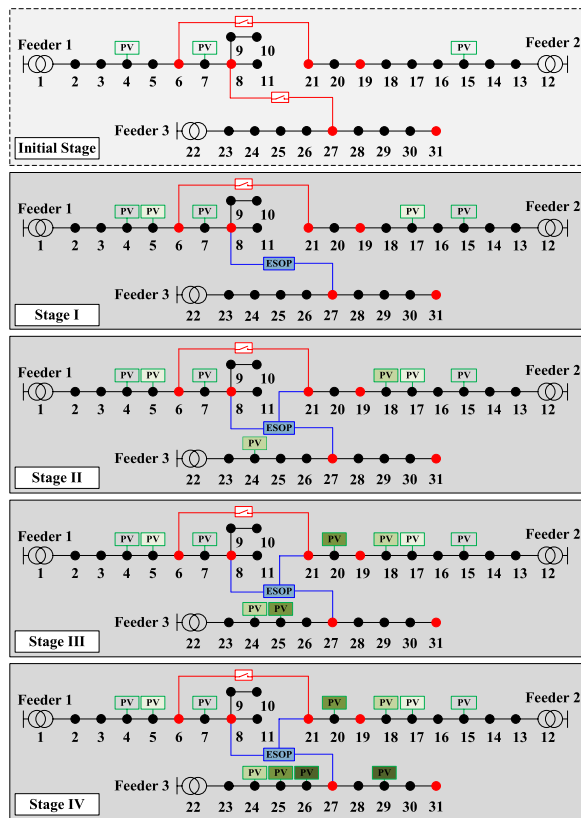


Fig. 8 Planning results of the network based on ESOP in Case V

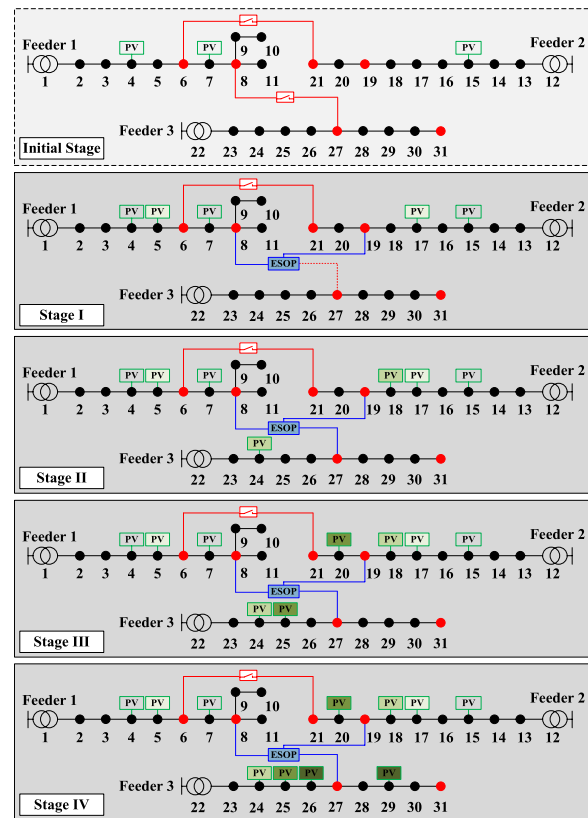


Fig. 9 Planning results of the network based on ESOP in Case VI

Table 9 Investment cost of multi-stage planning in Case VI

Price	Stage I	Stage II	Stage III	Stage IV
AC-DC converter price (RMB/kW)	1000	900	800	700
DC-DC converter price (RMB/kW)	500	450	420	400
Storage battery price (RMB/kWh)	500	450	420	400
Line constructing price (10 ⁴ RMB/km)	10	12	14	16

4.3.3 Price change of device investment

Further considering the price fluctuation of ESOP devices, the following case is added:

Case VI The multi-stage ESOP expansion planning is implemented by adopting the proposed planning method.

The planning results are given in Fig. 9 and the detailed planning investment cost is given in Table 9. At the first planning stage, a two-terminal ESOP is constructed between nodes 8 and 19, while at stage II, the third

Table 10 Multi-stage planning results in Case VI

Result	Stage I	Stage II	Stage III	Stage IV
AC-DC converter (MVA)				
Node 8	1.54	1.54	1.77	2.02
Node 19	0.51	0.51	2.09	2.13
Node 27	-	0.10	1.40	5.19
DC-DC converter (MW)	1.50	1.83	4.39	8.00
Storage battery (MWh)	4.38	5.19	16.77	45.16
ESOP investment cost (10 ⁴ RMB)	50.81	57.76	179.33	531.20
Total investment cost (10 ⁴ RMB)	155.52	172.06	323.74	768.72
Total cost (10 ⁴ RMB)	2709.54	2628.18	2267.60	1898.25

AC-DC converter is scheduled based on the existing two-terminal ESOP. The results indicate that the changes in equipment cost affect the formulation of ESOP expansion planning.

With a flat decline of price in Case VI, the initial scheduled ESOP investment cost reaches 5.08×10^5 RMB (from Table 10), which is much larger than the other cases. It is found that if the equipment cost cannot be reduced rapidly with the development, the investment of ESOP prefers to be concentrated in the early stages. Construction should be avoided during any period having an expensive and volatile price. In contrast, when the equipment cost is decreased, the expansion can be implemented to meet the future operational requirement in advance.

5 Conclusions

To address the flexible configuration of ESOP, this paper proposes a multi-stage ESOP expansion planning method with consideration of tie-line reconstruction. Considering the evolutionary relationship among different planning schemes, ESOP expansion can be implemented over a long time horizon. A cost–benefit analysis of multi-stage ESOP expansion planning is formulated. The results indicate that the total cost, including electricity purchase cost, voltage deviation cost, and DG curtailment cost, is reduced by 14.25% compared to the condition where no ESOP is allocated. In addition, the impact factors of ESOP planning are further analyzed. The results show that the reconstructed tie-lines contribute to the reduction of ESOP investment costs, while the need to allow for DG penetration is responsible for the scheduled scales of ESOP investment at different stages. Given price fluctuation, expansion should be avoided during the period having an expensive and volatile price. Through expanding ESOP in multiple stages, ESOP device utilization and the economy of the distribution network planning are significantly advanced.

Future investigation can be suggested as follows: first, the uncertainties of DG and load can be considered. These affect the results of ESOP planning. The integration of controllable devices brings enormous operational flexibility to ADNs. How to coordinate the planning of various devices will be further investigated to maximize the ESOP device utilization. In addition, the energy storage model and device lifecycle can be further analyzed.

Abbreviations

ADN: Active distribution network; ESOP: Energy storage integrated soft open point; SOP: Soft open point; ES: Energy storage; DG: Distributed generator; PV: Photovoltaic.

Sets

Ω_{all} : Set of all nodes; ℓ_{all} : Set of all lines; Ω_i : Set of nodes integrated converter in ESOP planning scheme k ; \mathcal{L} : Set of ESOP planning schemes; $\mathcal{L}(k)$: Set of

ESOP planning schemes evolved from scheme k ; $\mathcal{L}(k, \tau)$: Set of τ -terminal ESOP planning schemes evolved from scheme k .

Indices

i, j, g : Indices of nodes; k, h, p : Indices of ESOP planning schemes; r, r' : Indices of planning stages; ω : Index of clustering scenarios; t : Index of time instants; τ : Index of AC-DC converters in ESOP.

Variables

$P_{r,\omega,t,k,i}^{AC}$: Active/reactive power injection of ESOP at node i in scheme k and scenario ω at time t during stage r (kW, kvar); $Q_{r,\omega,t,k,i}^{AC}$: Active power loss of ESOP at node i in scheme k and scenario ω at time t during stage r (kW); $P_{r,\omega,t,k}^{ES}$: Active power injected and loss by ES of ESOP in scheme k and scenario ω at time t during stage r (kW); $P_{r,\omega,t,k}^{ESL}$: Capacity of AC-DC converter at node i in scheme k during stage r (kVA); $S_{r,k}^{AC}$: Energy stored by ES of ESOP in scheme k and scenario ω at time t during stage r (kWh); $S_{r,k}^{AC}, S_{r,k}^{DC}, S_{r,k}^{BA}$: Capacity of AC-DC /DC-DC /storage battery converters in scheme k during stage r (kVA); $P_{r,\omega,t,ij}$: Active/reactive power flow of line ij in scenario ω at time t during stage r (kW, kvar); $Q_{r,\omega,t,i}$: Total active/reactive power injection at node i in scenario ω at time t during stage r (kW, kvar); $V_{r,\omega,t,i}$: Squared voltage magnitude of node i and current magnitude of branch ij in scenario ω at time t during stage r (kV², A²); $P_{r,\omega,t,i}^{DG}$: Active/reactive power injection by DG at node i in scenario ω at time t during stage r (kW, kvar); $Q_{r,\omega,t,i}^{DG}$: Active/reactive power consumption at node i in scenario ω at time t during stage r (kW, kvar).

Parameters

N_t : Total number of planning stages; N_i : Total number of time instants; N_k : Total number of ESOP planning schemes; N_ω : Total number of clustering scenarios; T_r : Period of each planning stage; r_{ij}, x_{ij} : Resistance/reactance of line ij (Ω); A_{ac}, A_{dc} : Loss coefficient of AC-DC converter/DC-DC converter in ESOP; SOC_{min}^{ES} : Upper/lower limitations of state of charge of energy storage. SOC_{max}^{ES}

Acknowledgements

Not applicable

Author contributions

PL constructed the conceptualization and methodology of multi-stage expansion planning. JJ analyzed and interpreted the data. SC performed case studies, and contributed to writing the original draft of the manuscript. HJ was mainly responsible for reviewing and editing the manuscript. JX investigated the background of expansion planning technologies. GS provided the software support. JZ validated the rationality of the results. JW supervised the simulation experiments. CW was responsible for project administration. All authors read and approved the final manuscript.

Funding

This work was supported by the National Natural Science Foundation of China (51977139, 52061635103), Tianjin Science Foundation for Youths (21JCQNJC00430) and Science and Technology Project of State Grid Tianjin Electric Power Co. (KJ21-1–36).

Availability of data and materials

The datasets used and/or analyzed during the current study are available from the corresponding author on reasonable request.

Declarations

Competing interests

The authors declare that they have no known competing financial interests or personal relationships that could have appeared to influence the work reported in this paper.

Author details

¹Key Laboratory of Smart Grid of Ministry of Education, Tianjin University, Tianjin 300072, China. ²State Grid Kunshan Power Supply Company, Kunshan 215300, China. ³State Grid Tianjin Economic and Technological Research Institute, Tianjin 300171, China. ⁴Institute of Energy, School of Engineering, Cardiff University, Cardiff CF24 3AA, UK.

Received: 15 July 2022 Accepted: 28 October 2022

Published online: 11 November 2022

References

1. Erdiwansyah, M., Husin, H., Nasaruddin, M. Z., & Muhibbuddin, A. (2021). A critical review of the integration of renewable energy sources with various technologies. *Protection and Control of Modern Power Systems*, 6(3), 37–54.
2. Zhang, S., Cheng, H., Wang, D., Zhang, L., Li, F., & Yao, L. (2018). Distributed generation planning in active distribution network considering demand side management and network reconfiguration. *Applied Energy*, 228, 1921–1936.
3. Huang, K., Li, Y., Zhang, X., Liu, L., Zhu, Y., & Meng, X. (2021). Research on power control strategy of household-level electric power router based on hybrid energy storage droop control. *Protection and Control of Modern Power Systems*, 6(2), 178–190.
4. Sarantakos, I., Peker, M., Zografou-Barredo, N. M., Deakin, M., Patsios, C., Sayfutdinov, T., Taylor, P., & Greenwood, D. (2022). A robust mixed-integer convex model for optimal scheduling of integrated energy storage—soft open point devices. *IEEE Transactions on Smart Grid*.
5. Olujobi, O. J. (2020). The legal sustainability of energy substitution in Nigeria's electric power sector: Renewable energy as alternative. *Protection and Control of Modern Power Systems*, 5(4), 358–369.
6. Yang, Y., Wei, P., Huo, Q., Sun, J., & Xu, F. (2018). Coordinated planning method of multiple micro-grids and distribution network with flexible interconnection. *Applied Energy*, 228, 2361–2374.
7. You, R., & Lu, X. (2022). Voltage unbalance compensation in distribution feeders using soft open points. *Journal of Modern Power Systems Clean Energy*, 10(4), 1000–1008.
8. Huo, Y., Li, P., Ji, H., Yan, J., Song, G., Wu, J., & Wang, C. (2021). Data-driven adaptive operation of soft open points in active distribution networks. *IEEE Transactions on Industrial Informatics*, 17(12), 8230–8242.
9. Zhang, S., Fang, Y., Zhang, H., Cheng, H., & Wang, X. (2022). Maximum hosting capacity of photovoltaic generation in SOP-based power distribution network integrated with electric vehicles. *IEEE Transactions on Industrial Informatics*.
10. Pamshetti, V. B., Singh, S., Thakur, A. K., & Singh, S. P. (2021). Multistage coordination Volt/VAR control with CVR in active distribution network in presence of inverter-based DG units and soft open points. *IEEE Transactions on Industry Applications*, 57(3), 2035–2047.
11. Wang, C., Song, G., Li, P., Ji, H., Zhao, J., & Wu, J. (2017). Optimal siting and sizing of soft open points in active electrical distribution networks. *Applied Energy*, 189, 301–309.
12. Cong, P., Hu, Z., Tang, W., Lou, C., & Zhang, L. (2020). Optimal allocation of soft open points in active distribution network with high penetration of renewable energy generations. *IET Generation, Transmission and Distribution*, 14, 6732–6740.
13. Wang, J., Zhou, N., Chung, C. Y., & Wang, Q. (2020). Coordinated planning of converter-based DG units and soft open points incorporating active management in unbalanced distribution networks. *IEEE Transaction on Sustainable Energy*, 11(3), 2015–2027.
14. Yang, X., Zhou, Z., Zhang, Y., Liu, J., Wen, J., Wu, Q., & Cheng, S. (2022). Resilience-oriented co-deployment of remote-controlled switches and soft open points in distribution networks. *IEEE Transaction on Power System*.
15. Zhang, J., Foley, A., & Wang, S. (2021). Optimal planning of a soft open point in a distribution network subject to typhoons. *International Journal of Electrical Power & Energy Systems*, 129, 106839.
16. Qin, Q., Han, B., Li, G., Wang, K., Xu, J., & Luo, L. (2022). Capacity allocations of SOPs considering distribution network resilience through elastic models. *International Journal of Electrical Power & Energy Systems*, 134(3), 107371.
17. Wang, X., Guo, Q., Tu, C. M., Che, L., Yang, W. L., Xiao, F., & Hou, Y. C. (2022). A two-layer control strategy for soft open points considering the economical operation area of transformers in active distribution networks. *IEEE Transaction on Sustainable Energy*.
18. He, Y., Wu, H., Bi, R., Qiu, R., Ding, M., Sun, M., Xu, B., & Sun, L. (2022). Coordinated planning of distributed generation and soft open points in active distribution network based on complete information dynamic game. *International Journal of Electrical Power & Energy Systems*, 138, 107953.
19. Liu, S., Zhou, C., Guo, H. M., Shi, Q. X., Song, T. C. E., Schomer, I., & Liu, Y. (2021). Operational optimization of a building-level integrated energy system considering additional potential benefits of energy storage. *Protection and Control of Modern Power Systems*, 6(4), 55–64.
20. Magdy, G., Bakeer, A., & Alhasheem, M. (2021). Superconducting energy storage technology-based synthetic inertia system control to enhance frequency dynamic performance in microgrids with high renewable penetration. *Protection and Control of Modern Power Systems*, 6(36), 1–13.
21. Bai, L., Jiang, T., Li, F., Chen, H., & Li, X. (2018). Distributed energy storage planning in soft open point based active distribution networks incorporating network reconfiguration and DG reactive power capability. *Applied Energy*, 210, 1082–1091.
22. Fu, X., Wu, X., Zhang, C., Fan, S., & Liu, N. (2022). Planning of distributed renewable energy systems under uncertainty based on statistical machine learning. *Protection and Control of Modern Power Systems*, 7(41), 1–27.
23. He, W., King, M., Luo, X., Dooner, M., Li, D., & Wang, J. (2021). Technologies and economics of electric energy storages in power systems: Review and perspective. *Advance in Applied Energy*, 4, 100060.
24. Tabares, A., Franco, J. F., Lavorato, M., & Rider, M. J. (2016). Multistage long-term expansion planning of electrical distribution systems considering multiple alternatives. *IEEE Transactions on Power Systems*, 31, 1900–1914.
25. Bhattiprolu, P. A., & Conejo, A. J. (2022). Multi-period AC/DC transmission expansion planning including shunt compensation. *IEEE Transactions on Power Systems*, 37(3), 2164–2176.
26. Ding, T., Qu, M., Huang, C., Wang, Z., Du, P., & Shahidehpour, M. (2021). Multi-period active distribution network planning using multi-stage stochastic programming and nested decomposition by SDDIP. *IEEE Transactions on Power Systems*, 36(3), 2281–2292.
27. Peña, A. A., Romero-Quete, D., & Cortes, C. A. (2022). Sizing and siting of battery energy storage systems: A Colombian case. *Journal of Modern Power Systems Clean Energy*, 10(3), 700–709.
28. Wei, P., Xue, Z., Wei, D., Tang, C., & Yao, L. (2022). Review of operational control strategy for dc microgrids with electric-hydrogen hybrid storage systems. *CSEE Journal of Power Energy System*, 8, 329–346.
29. Qi, Q., Long, C., Wu, J., & Yu, J. (2018). Impacts of a medium voltage direct current link on the performance of electrical distribution networks. *Applied Energy*, 230, 175–188.
30. Liu, H., Deng, Z., Li, X., Guo, L., Huang, D., Fu, S., Chen, X., & Wang, C. (2020). The averaged-value model of flexible power electronics substation in hybrid AC/DC distribution systems. *CSEE Journal of Power Energy System*, 8, 452–464.
31. Huo, Y., Li, P., Ji, H., Yu, H., Yan, J., Wu, J., & Wang, C. (2022). Data-driven coordinated voltage control method of distribution networks with high DG penetration. *IEEE Transactions on Power Systems*. <https://doi.org/10.1109/TPWRS.2022.3172667>
32. Schleifer, A. H., Murphy, C. A., Cole, W. J., & Denholm, P. L. (2021). The evolving energy and capacity values of utility-scale PV-plus-battery hybrid system architectures. *Advance in Applied Energy*, 2, 100015.

33. Saboori, H., Hemmati, R., & Abbasi, V. (2015). Multistage distribution network expansion planning considering the emerging energy storage systems. *Energy Conversion and Management*, *105*, 938–945.
34. Suthar, S., & Pindoriya, N. M. (2020). "Energy management platform for integrated battery-based energy storage – solar PV system: A case study. *IET Energy System Integration*, *2*, 373–381.
35. Ji, H., Wang, C., Li, P., Ding, F., & Wu, J. (2019). Robust operation of soft open points in active distribution networks with high penetration of photovoltaic integration. *IEEE Transaction on Sustainable Energy*, *10*, 280–289.
36. Chiou, J. P., Chang, C. F., & Su, C. T. (2005). Variable scaling hybrid differential evolution for solving network reconfiguration of distribution systems. *IEEE Transactions on Power Systems*, *20*(2), 668–674.
37. Zhao, J., Chen, H., Song, G., Fan, X., Li, P., & Wu, J. (2022). Planning method of soft open point in distribution network considering reliability benefits. *Automation of Electric Power Systems*, *44*, 22–31.
38. Shu, Y., Zhang, L., Zhang, Y., Wang, Y., Lu, G., Yuan, B., et al. (2021). Carbon peak and carbon neutrality path for China's power industry. *Strategic Study of CAE*, *23*, 1–14.
39. Liu, D., Zhang, S., Cheng, H., Liu, L., Zhang, J., & Zhang, X. (2021). Reducing wind power curtailment by risk-based transmission expansion planning. *International Journal of Electrical Power & Energy Systems*, *124*, 106349.

Submit your manuscript to a SpringerOpen[®] journal and benefit from:

- ▶ Convenient online submission
- ▶ Rigorous peer review
- ▶ Open access: articles freely available online
- ▶ High visibility within the field
- ▶ Retaining the copyright to your article

Submit your next manuscript at ▶ [springeropen.com](https://www.springeropen.com)
